Ceramics International xxx (xxxx) xxx–xxx

Contents lists available at ScienceDirect

Ceramics International

journal homepage: www.elsevier.com/locate/ceramint

Thermoelectric properties and figure of merit of perovskite-type $Sr_{1-x}La_xSnO_3$ ceramics

Masahiro Yasukawa[a,*], Kazushige Ueda[b], Satoru Fujitsu[c], Hideo Hosono[c,d]

[a] Department of Social Design Engineering, National Institute of Technology, Kochi College, 200-1 Monobe, Nankoku 783-8508, Japan
[b] Department of Materials Science, Kyushu Institute of Technology, 1-1 Sensui, Tobata, Kitakyushu 804-8550, Japan
[c] Materials Research Center for Element Strategy, Tokyo Institute of Technology, 4259 Nagatsuta, Midori, Yokohama 226-8503, Japan
[d] Laboratory for Materials and Structures, Tokyo Institute of Technology, 4259 Nagatsuta, Midori, Yokohama 226-8503, Japan

ARTICLE INFO

Keywords:
C. Electrical conductivity
C. Thermal conductivity
C. Thermoelectric properties
D. Perovskites

ABSTRACT

The thermoelectric properties of perovskite-type $Sr_{1-x}La_xSnO_3$ ceramics with x=0.01–0.05 were evaluated from the Seebeck coefficient *S*, electrical conductivity σ, and thermal conductivity κ measured at high temperatures. The La-doped ceramics were *n*-type semiconductors exhibiting thermally activated electrical conduction behaviors in the temperature range of 473–1073 K. Eelectron carriers were introduced into the conduction band from doped La atoms up to x=0.03, which was the solubility limit of La at Sr site. The temperature dependence of the κ values for the ceramics was unaffected by both the La content and the microstructures. Estimations of the electronic thermal conductivities by the Wiedemann-Franz law revealed that the phonon thermal conductivities were dominant for all ceramics. The dimensionless figure of merit *ZT* increased with increasing temperature for all ceramics and reached 0.02–0.05 at 1073 K. In contrast to cubic $Ba_{1-x}La_xSnO_3$ ceramics, bending of the Sn–O–Sn bonds due to octahedral tilting distortion in $Sr_{1-x}La_xSnO_3$ lowered the electron mobility, decreasing the power factor $S^2\sigma$ and *ZT* values, although it effectively reduced the phonon mean free path, decreasing the κ values.

1. Introduction

Thermoelectric oxide materials, which have high thermal and chemical stabilities at high temperatures in air, are expected to convert high temperature waste heat from incinerators or combustion engines into electricity. The development of high-performance thermoelectric oxides is important for a high-conversion efficiency from heat to electricity. The thermoelectric performance of a material is usually evaluated by the figure of merit *Z*, which is expressed as $Z=S^2\sigma\kappa^{-1}$, where *S* is the Seebeck coefficient, σ is the electrical conductivity, and κ is the thermal conductivity. The $S^2\sigma$ value, namely the power factor, is also used as a rough estimate of the performance. A criterion for the practical use of a thermoelectric material is $ZT=1$ where *T* is the absolute temperature and *ZT* is known as dimensionless figure of merit. Although good thermoelectric materials are known for *n*-type and *p*-type conducting oxides [1–9], it is still a challenging subject to find novel high-performance thermoelectric oxides.

Alkaline earth stannates $ASnO_3$ (A=Ba, Sr, Ca) are perovskite-type oxides which consist of A-site alkaline earth ions and three-dimensional linkages of SnO_6 octahedra sharing their vertex oxygens [10–14]. $BaSnO_3$ is a primitive cubic perovskite with straight linkages of Sn–O–Sn bonds, while $SrSnO_3$ and $CaSnO_3$ have orthorhombic lattices with zigzag linkages of Sn–O–Sn bonds due to SnO_6 octahedral tilting [12–14]. We have reported the thermoelectric properties and the figure of merit of La-doped $BaSnO_3$ ceramics at high temperatures [15,16]. $Ba_{1-x}La_xSnO_3$ ceramics exhibit *n*-type degenerate semiconducting behavior, and the highest *ZT* value of ~0.1 occurs at 1073 K for ceramics with low La contents x=0.002 and x=0.005. To explore higher *ZT* values in $ASnO_3$, the thermoelectric properties should be investigated in $SrSnO_3$ or $CaSnO_3$. $SrSnO_3$ is originally an electrical insulator, but it becomes a semiconductor when doped with Sb at the Sn sites or with Ln such as La, Nd, and Er at the Sr sites [17–23].

In this study, $Sr_{1-x}La_xSnO_3$ ceramics with x=0.00–0.05 are prepared, and their electrical conductivity, Seebeck coefficient, and thermal conductivity are measured at high temperatures to elucidate the thermoelectric properties and figure of merit.

2. Experimental

$Sr_{1-x}La_xSnO_3$ ceramics were prepared by a polymerized complex method followed by a spark plasma sintering (SPS) technique. Reagents of $Sr(NO_3)_2$ (98%), $LaCl_3{\cdot}7H_2O$ (97%), and $SnCl_2{\cdot}2H_2O$

* Corresponding author.
E-mail address: myasukawa@ms.kochi-ct.ac.jp (M. Yasukawa).

http://dx.doi.org/10.1016/j.ceramint.2017.04.136
Received 11 March 2017; Received in revised form 20 April 2017; Accepted 24 April 2017

(97%) (Kishida Chemical) were weighed stoichiometrically with La contents of x=0.00, 0.01, 0.03, or 0.05, and dissolved in ethylene glycol (EG). The concentration of Sn was fixed at 0.25 M. The metal solution in EG was mixed with a citric acid solution in ethanol (1 M) and stirred at 353 K for 1 h to prepare a transparent solution of metal citrate complexes. Then the solution was heated at 408 K for 28 h to form a brownish solution of polymerized citrate complexes. The solution was gelatinized by vacuum evaporation of residual EG at 373 K and pyrolyzed at 623 K in air to form a black solid precursor. The precursor was heated at 1173 K for 3 h, and then fired at 1473 K for 10 h in an air-flow to form a fine powder of perovskite-type $Sr_{1-x}La_xSnO_3$. The fine powder was mounted into a carbon die and sintered at 1373 K for 10 min in a vacuum of ~5 Pa by SPS (SPS SYNTEX, SPS-511S).

The sintered polycrystalline ceramics were evaluated by X-ray powder diffraction (XRD) measurements with CuKα radiation (Rigaku, RINT-UltimaIII) to identify the phases in the ceramics and to estimate the lattice parameters. The relative density of the ceramics was estimated as the ratio of the measured bulk density to the theoretical one; the former was estimated from the mass and volume of the ceramics, while the latter was estimated from the lattice parameters assuming a stoichiometric composition of $Sr_{1-x}La_xSnO_3$. The microstructure of the ceramics was observed by scanning electron microscopy (JEOL, JSM-6610). Using laboratory-made equipment, the electrical conductivity and Seebeck coefficient were measured at several temperatures from 1073 K to 473 K in air on rectangular-shaped samples. The former data were obtained by the direct current four-probe method and the latter data were obtained by correcting the linear gradient of $\Delta V/\Delta T$ for the thermopower of platinum [24]. ΔV and ΔT are the thermoelectromotive force and temperature difference between the two ends of the sample measured with Pt wires and Pt/Pt-Rh thermocouples, respectively. ΔT was controlled in a range of ~5 K, and about 10 sets of ΔV and ΔT were measured. The thermal diffusivity and specific heat were measured in the temperature range of 300–1073 K by the laser flash method (ULVAC-RIKO, TC-9000), and the thermal conductivity was estimated as the product of the bulk density, thermal diffusivity, and specific heat.

3. Results and discussion

Fig. 1(a) shows the XRD patterns for the SPS-treated $Sr_{1-x}La_xSnO_3$ ceramics with x=0.00, 0.01, 0.03, and 0.05. The XRD patterns for the samples with x=0.00–0.03 are completely indexed with the powder diffraction data of orthorhombic $SrSnO_3$ [12], but the XRD pattern for the sample with x=0.05 shows additional diffraction peaks from a secondary phase $La_2Sn_2O_7$. Therefore, the samples with x=0.00, 0.01, and 0.03 are perovskite-type single phases of $Sr_{1-x}La_xSnO_3$, while the sample with x=0.05 includes a small amount of $La_2Sn_2O_7$. Fig. 1(b) shows the La content dependence of orthorhombic lattice parameters a, b, and c. The values are plotted as $a\times\sqrt{2}$, $b\times\sqrt{2}$, and c. All the values increase as the La content increases and become saturated at x=0.03. These XRD results indicate that the solubility limit of La at Sr site is approximately x=0.03. The relative densities are estimated to be ≥95% for the single-phase ceramics of x=0.00–0.03. Fig. 2 shows the SEM images for the fractured surfaces of the $Sr_{1-x}La_xSnO_3$ ceramics. The SEM images confirm that all the ceramics with x=0.00–0.05 prepared by the SPS treatment have well-densified microstructures and that the grain sizes decrease as the La content increases; grain sizes are several microns to 10 μm for x=0.00 and sub-microns for x=0.05. This result suggests that grain growth during sintering is suppressed with increasing La content, although the mechanism is unclear.

Fig. 3(a) shows the reciprocal temperature dependence of the electrical conductivity σ for $Sr_{1-x}La_xSnO_3$ ceramics with x=0.01, 0.03, and 0.05. The σ values increase with increasing temperature for all the ceramics. The values also increase as the La content increase from x=0.01 to x=0.03, but become saturated at x=0.03. Fig. 3(b) shows the temperature dependence of the Seebeck coefficient S for the

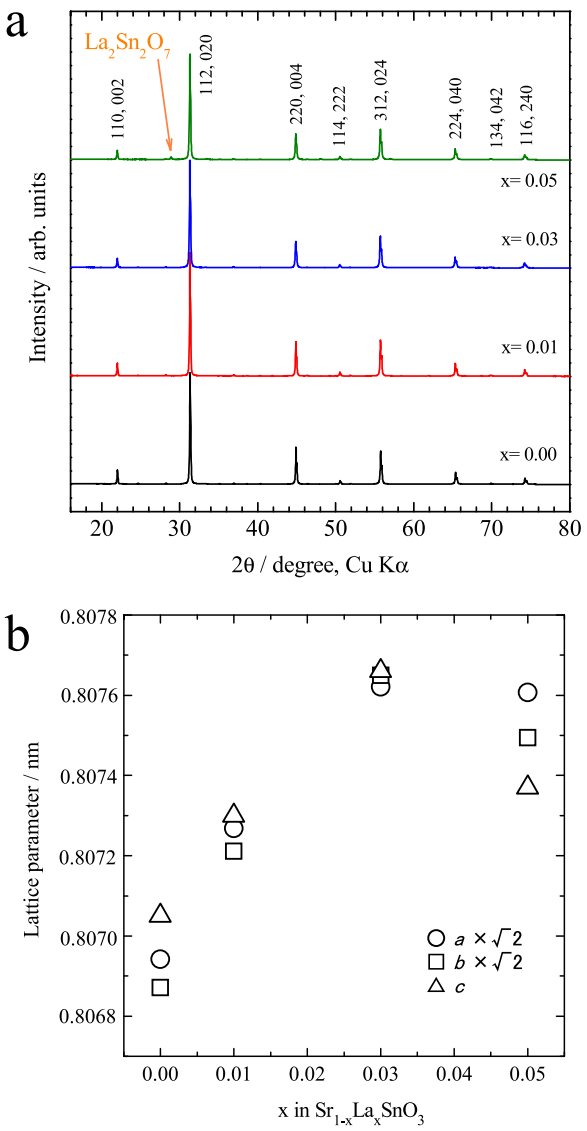

Fig. 1. (a) XRD patterns for $Sr_{1-x}La_xSnO_3$ ceramics with x=0.00, 0.01, 0.03, and 0.05 after the SPS treatment. (b) La content dependence of the lattice parameters a, b, and c for $Sr_{1-x}La_xSnO_3$. Circles, squares, and triangles are plotted as the values for $a\times\sqrt{2}$, $b\times\sqrt{2}$, and c, respectively.

$Sr_{1-x}La_xSnO_3$ ceramics with x=0.01, 0.03, and 0.05. For all the ceramics, the S values are negative and linearly depend on the temperature. The absolute S values decrease as the La content increases from x=0.01 to x=0.03 and almost become saturated at x=0.03. The La content dependence of the σ and S values indicates that the electron carriers are generated from the doped La atoms up to approximately x=0.03, which is the solubility limit of La at the Sr sites. The La doping of x=0.03 yields a calculated electron carrier density of ~5×10^{20} cm^{-3} when a La ion at the Sr site generates one electron carrier.

The linear temperature dependence of the S values indicates that the electron carriers in the $Sr_{1-x}La_xSnO_3$ ceramics are degenerate to the conduction band (CB); the electron carriers generated from the La ions are introduced into the CB composed of Sn5s–O2p σ^* anti-bonding orbitals and the Fermi level (E_F) is located above the CB minimum. However, the thermal activation-type behavior of the σ values is observed for the $Sr_{1-x}La_xSnO_3$ ceramics. This behavior can be attributed to the SnO_6 octahedral tilting distortion, that is, the bending of the Sn–O–Sn bonds. The electron carriers are introduced from the La ions into the CB, but the electron mobility should decrease due to the smaller overlap between Sn5s and O2p orbitals compared with that